

THE TREATMENT OF NUCLEAR EFFECTS FOR NEUTRINO INTERACTIONS IN THE FLUKA CODE*

G. BATTISTONI, P.R. SALA

INFN, Sezione di Milano, Via Celoria 16, 20133 Milan, Italy

A. FERRARI

CERN, CH-1211 GENÈVE 23, Switzerland

(Received June 23, 2006)

FLUKA is a general purpose Monte Carlo code for transport and interaction of particles. In particular it contains detailed nuclear models which have been successfully tested in hadronic interactions. The same approach can be successfully applied to neutrino interactions. Here we review the main features of the FLUKA nuclear models and their application to the generations of interactions of neutrinos with $E \geq 100$ MeV and proton decay.

PACS numbers: 13.15.+g, 25.30.Pt, 21.60.Ka, 24.10.Lx

1. Introduction

The achievement of a reasonable Monte Carlo approach to nuclear effects in neutrino interactions is considered an essential step to build reliable analysis tools for the next generation neutrino experiments. The same effects must also be considered for proton decay event generators. Here we present a summary of the main features of the well established and tested nuclear “environment” of the Monte Carlo FLUKA code. We refer to the literature [1] for a general description of FLUKA. In the following we give some details about the features of the nuclear model of FLUKA relevant to ν interactions. Then we present a summary of the main conclusions resulting from the coupling of FLUKA with “free” ν -nucleon event generators, as presented, for instance, in [2].

* Presented at the XX Max Born Symposium “Nuclear Effects in Neutrino Interactions”, Wrocław, Poland, December 7–10, 2005.

2. The nuclear model of FLUKA: PEANUT

The intermediate energy hadronic model of FLUKA is called PEANUT. Presently, PEANUT handles interactions of nucleons, pions, kaons, and γ rays from a few GeV down to reaction threshold (or 20 MeV for neutrons). The reaction mechanism is modeled in PEANUT by an explicit Generalized INtranuclear Cascade (GINC) smoothly joined to statistical (exciton) pre-equilibrium emission [3, 4]. At the end of the GINC and exciton chain, the evaporation of nucleons and light fragments (α , d , ${}^3\text{H}$, ${}^3\text{He}$) is performed, following the Weisskopf [5] treatment. Competition of fission with evaporation has been implemented, again within a statistical approach. For light nuclei, the so called Fermi Break-up model [6, 7] is used instead. The excited nucleus is supposed to disassemble just in one step into two or more fragments, with branching given by plain phase space considerations, corrected for Coulomb barriers when applicable. The excitation energy still remaining after (multiple) evaporation is dissipated via emission of γ rays [8]. The GINC proceeds through hadron multiple collisions in a cold Fermi gas. The hadron–nucleon cross sections used in the calculations are the free ones modified by Pauli blocking, except for pions and negative kaons that deserve a special treatment. The Fermi motion is taken into account, both to compute the interaction cross section, and to produce the final state particles.

Secondaries are treated exactly like primary particles, with the only difference that they start their trajectory already inside the nucleus. Primary and secondary particles are transported according to their nuclear mean field and to the Coulomb potential. All particles are transported along classical trajectories, nevertheless a few relevant quantistic effects are included.

Binding Energies (B_{en}) are obtained from mass tables, depending on particle type and on the actual composite nucleus, which may differ from the initial one in case of multiple particle emission. Relativistic kinematics is applied, with accurate conservation of energy and momentum, and with inclusion of the recoil energy and momentum of the residual nucleus. In both stages, INC and exciton, the nucleus is modeled as a sphere with density given by a symmetrized Woods–Saxon [9] shape for $A > 16$ and by a harmonic oscillator shell model for light isotopes (see [10]). Proton and neutron densities are generally different, according again to shell model ones for $A < 16$, and to the droplet model [11] for heavier nuclei.

A standard position dependent Fermi momentum distribution is implemented in PEANUT up to a local Fermi momentum $k_{\text{F}}(r)$ given by

$$k_{\text{F}}^{p,n}(r) = (3\pi^2 \rho^{p,n}(r))^{1/3}, \quad (1)$$

where $\rho^{p,n}$ is the neutron or proton density as defined in the previous paragraph. Fermi momentum is smeared according to the uncertainty principle

assuming a position uncertainty = $\sqrt{2}$ fm. The potential depth felt by nucleons at any radius r is given by the Fermi energy plus the relevant binding energy.

Positive Kaons are an excellent probe to test the Fermi distribution. They undergo only elastic and charge exchange scattering up to ≈ 800 MeV/ c , and their interactions are easily modeled starting from phase shift analysis. A nice comparison of PEANUT and data on K^+ Pb scattering is shown in Fig. 1: the width of these distributions is totally determined by Fermi momentum. For pions, a nuclear potential has been calculated starting from the standard pion–nucleus optical potential [13].

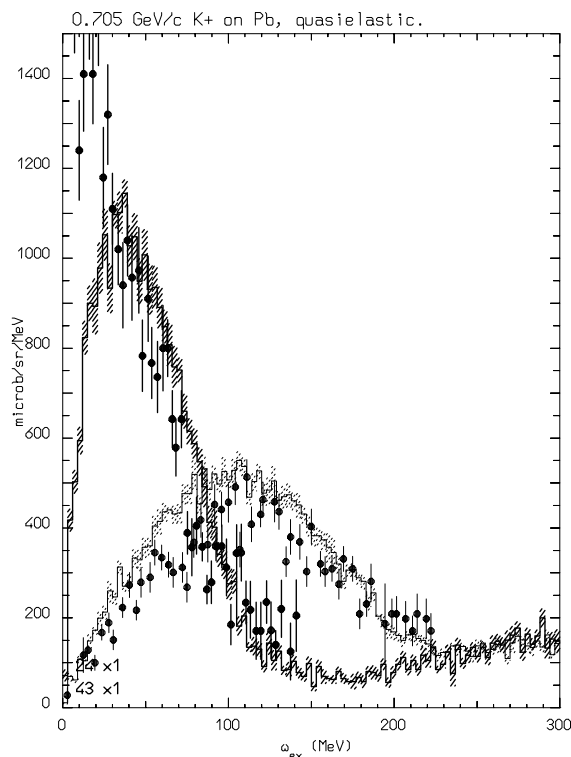


Fig. 1. (K^+, K^{*+}) on Pb versus residual excitation, 705 MeV/ c , at 24° and 43° . Histogram: FLUKA, dots: data [12]. Elastic scattering is not included in the calculations. On free nucleon the recoil energy is 43 MeV at 24° , 117 MeV at 43° .

Pion induced reactions are complex, mainly because of two- and three-nucleon absorption processes. Above the pion production threshold, the inelastic interactions are handled by a resonance model. Other pion–nucleon interactions proceed through the non-resonant channel and the p -wave chan-

nel with the formation of a Δ resonance. In nuclear matter, the Δ can either decay, resulting in elastic scattering or charge exchange, or interact with other nucleons, resulting in pion absorption. The width of the resonance is thus different from the free one. To account for this we made use of the approach outlined in [15], where the partial widths for quasi-elastic scattering, two body and three body absorption are considered. Isospin relations have been extensively applied both to derive the pion–nucleon cross sections in any given charge configuration from the three experimentally known, and to weight the different interaction and decay channels of the Δ resonance [14,16].

Angular distributions of reaction products are sampled according to experimental data both for pion scattering (from free pion–nucleon) and pion absorption (from absorption on ^3He and deuterium).

The naive use of free hadron–nucleon cross sections would lead to hadron mean free paths in nuclei by far too short with respect to reality. Indeed there are many effects that influence the in-medium cross sections, and some of them are accounted for in FLUKA.

1. Pauli blocking: any secondary nucleon created in an intranuclear interaction must obey the Pauli exclusion principle, thus it must have enough energy to jump above the Fermi level. For ν interactions, this results in a reduction of the cross section with respect to the free one. The effect is important at low ν energies, and is stronger for $\bar{\nu}$ due to the lower average q^2 .
2. Nucleon antisymmetrization effects [17], which decrease the probability for secondary particles to reinteract on a nucleon of the same type very close to the production point
3. Nucleon–nucleon hard-core correlations which also prevent secondary particles to collide again too close to the production point. Typical hard-core radii used are in the range 0.5–1 fm.
4. Formation zone and coherence length. The formation zone [18] concept after pion or nucleon interactions has a privileged status among quantistic effects. It can be understood considering that hadrons are composite objects and that the typical time of strong interactions is of the order of 1 fm. If one thinks about the hadrons emerging from an inelastic interaction, it requires some time to them to “materialize” and be able to undergo further interactions. This time interval can be expressed as

$$t_{\text{lab}} \approx \frac{\hbar E_{\text{lab}}}{p_{\text{T}}^2 + M^2}. \quad (2)$$

In the FLUKA implementation, the transverse energy entering in Eq. (2) is relative to the jet axis, not to the projectile direction. In case of elastic or quasi-elastic interactions a more rigorous approach can be followed. The “coherence” length after (quasi)elastic or charge exchange scatterings is analogue to the formation zone concept, such interactions cannot be localized better than the position uncertainty connected with the four-momentum transfer of the collision. Reinteractions occurring at distances shorter than the coherence length would undergo interference and cannot be treated anyway as independent interactions on other nucleons. The coherence length is the analogue of the formation time concept for elastic or quasi-elastic interactions and can be applied to the secondaries produced in quasi-elastic neutrino–nucleon interactions.

3. Application of FLUKA to neutrino interaction

In the framework of the work for the ICARUS experiment [19], FLUKA has been coupled to a quasi-elastic neutrino generator based on [20], and to the NUX model [21], mainly for deep inelastic scattering. The NUX-FLUKA combination has successfully simulated data from the NOMAD experiment at CERN. From this experience, we have learned about the effects of reinteractions in the nucleus. These may be summarized as follows.

The large cross section for pion absorption in the Δ region can change dramatically the kinematics of ν interactions. As an example, For 1 GeV ν_μ energy, only 55% of the produced π escape from a Fe nucleus, and 75% from an oxygen nucleus. Reinteractions *increase* the hadron multiplicity with respect to the initial state kinematics, due to the buildup in the intranuclear cascade. An increase in the formation zone corresponds to a suppression of the high multiplicity tail. Reinteractions *populate* the hadron spectrum in the 100 MeV kinetic energy range, *i.e.* the *cascade* particles, and in the evaporation peak. As an example, for 10 GeV ν_μ on ^{16}O , the introduction of the formation zone suppresses the cascade particles by about 40%; additional variations of a factor two have effects of the order of 15%. Reinteractions *depopulate* the hadron spectrum for $p \gtrsim 1$ GeV/ c . In the same test case, the decrease is around 20%. The formation zone approximately halves this percentage. Reinteractions *increase* the average emission angle, even for the high energy part of the spectrum. The “standard” formation zone decreases the average hadron emission angle by 10% for $p > 0.2$ GeV/ c , and by 4% for $p > 2$ GeV/ c (both for 10 GeV ν_μ on ^{16}O). The reconstruction of kinematic variables is affected by nuclear effects. In this respect it is important to distinguish two detector “families”: water Cerenkov and fine-grained detectors.

A first item is channel identification. In a fine grained detector, Charged Current (CC) Quasi Elastic (QE) reactions are identified by the presence of one lepton and one proton above threshold. The acceptance of this identification depends on the experimental threshold and on nuclear effects. Proton threshold acts differently for bound and free target, and even in the absence of reinteractions there is a small effect due to nuclear binding. When looking at “single pion” reactions, identified as events with one lepton, and one pion above threshold, the effect of reinteractions becomes dramatic, around 50% of events are lost for 1 GeV ν_μ on Fe even at zero threshold, and 25% on oxygen; it decreases slowly with increasing ν energy, reaching 40% (20%) at 10 GeV on Fe (oxygen). These “lost” events are, however, not really lost, but only borrowed by other channels. It can be seen that almost all the events lost in the one-pion channel populate the QE channel. The situation is similar in the case of a water Cerenkov detector, where the QE CC are “single ring” and the single π is seen as a lepton ring plus one pion.

Reconstruction of the incident ν energy is logically the second essential step. In QE CC reactions, the incident neutrino energy E_ν can be derived from the lepton energy E_l and emission angle θ . Fig. 2 shows the reconstructed E_ν for 1 GeV ν_μ on oxygen, assuming water Cerenkov cuts.

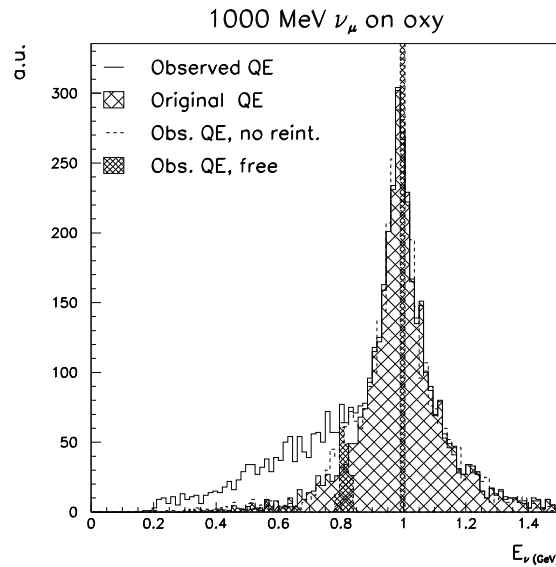


Fig. 2. Reconstructed ν energy from QE CC events, for 1 GeV ν_μ on ^{16}O or free neutrons, assuming Cerenkov cuts.

The distribution marked as “original” QE events, is obtained by accepting the events flagged as QE by the generator. The spread due to the target Fermi motion is evident. Note that in FLUKA, there is no other nuclear

effect on the lepton, except for Coulomb deflection. The continuous curve is built with the events identified as QE. The tail on the left is due to misidentified events. The dotted curve is again the identified QE, but with reinteractions switched off; as expected, the tail disappears, but not completely, and there is still a small bump of misidentified events. This small contribution is present also in the case of a reaction on a free nucleon, and is due to the experimental threshold on pion detection. In the case of a non monochromatic beam, the net effect is an enhancement of the low energy part of the reconstructed spectrum with respect to the true one.

Additional items are the Q^2 and the missing transverse momentum reconstruction. We present in Fig. 3 the Cerenkov-like reconstructed Q^2 distribution from 1 GeV ν_μ on oxygen.

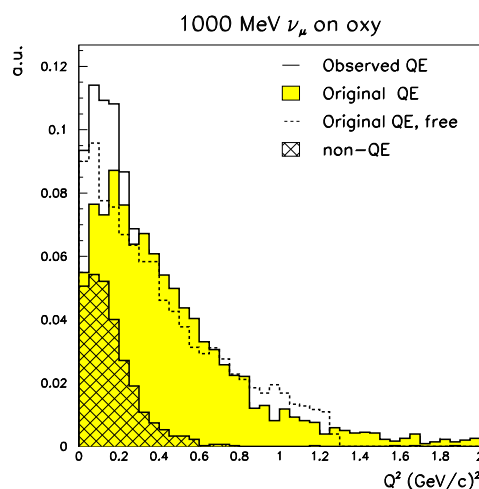


Fig. 3. Reconstructed Q^2 in the QE CC interactions of 1 GeV ν_μ on ^{16}O .

A suppression of the low Q^2 events is evident, due to Pauli blocking. High Q^2 tails come from Fermi motion, but are partially suppressed when the proton is above threshold. The misidentified non QE events populate mainly the medium-low part. The net suppression of the low Q^2 with respect to the distribution peak is of the order of 20%. The total transverse momentum of the reaction products is a key kinematic quantity, for instance for τ identification. At low ν energy p_T^{miss} is dominated, already in the initial state, by the effect of Fermi motion. There is a high p_T tail due to reinteractions, that is, however, smaller than the broadening due to instrumental effects. At higher energies, the reinteraction tail is more important, but the distribution can be completely masked by imprecision of event reconstruction.

Hadron multiplicity is often assumed as a good probe of Monte Carlo accuracy. Indeed high multiplicity events are generated by reinteractions. A correct simulation of final state effects, and in particular of the formation zone, is essential to reproduce experimental data. On the other hand, experimental multiplicities and hadron spectra are an unique tool to fix the scale of the formation zone in ν interactions, that could be in principle different from the one active in hadron–nucleus reactions.

4. Conclusions

The FLUKA nuclear interaction model has capabilities which have been successfully tested in hadron and photon induced reactions. We have applied the same models to the generation of neutrino interactions on single nucleons and proton decay. In these context, nuclear effects, both on initial state and on final state, affect all kinematic quantities. In the future, the FLUKA models will be coupled to more refined neutrino event generators more suitable for very low neutrino energy and Q^2 values, as those based on RPA principles.

REFERENCES

- [1] A. Ferrari, P.R. Sala, A. Fassò, J. Ranft, CERN-2005-010, INFN/TC_05/11 (2005); A. Ferrari, P.R. Sala, A. Fassò, J. Ranft, Proc. of CHEP2003, eConf C0303241, (2003) [[hep-ph/0306267](#)].
- [2] G. Battistoni, A. Ferrari, A. Rubbia, P.R. Sala, The FLUKA nuclear cascade model applied to neutrino interaction, Proceedings of the “Second International Workshop on Neutrino-Nucleus Interactions in the few-GeV Region, NUINT02, December 2002, University of California, Irvine, USA.
- [3] E. Gadioli, P.E. Hodgson, *Pre-Equilibrium Nuclear Reactions*, Clarendon Press, Oxford 1992.
- [4] J.J. Griffin, *Phys. Rev. Lett.* **17**, 438 (1966).
- [5] V.F. Weisskopf, *Phys. Rev.* **52**, 295 (1937).
- [6] E. Fermi, *Prog. Theor. Phys.* **5**, 1570 (1950).
- [7] M. Epherre, E. Gradsztajn, *J. Physique* **18**, 48 (1967).
- [8] A. Ferrari, P.R. Sala, J. Ranft, S. Roesler, *Z. Phys.* **C71**, 75 (1996).
- [9] M.E. Grypeos, G.A. Lalazassis, S.E. Massen, C.P. Panos, *J. Phys. G* **17**, 1093 (1991).
- [10] L.R.B. Elton, *Nuclear Sizes*, Oxford University Press, Oxford 1961.
- [11] W.D. Myers, *Nucl. Phys.* **A204**, 465 (1973); W.D. Myers, *Droplet Model of Atomic Nuclei*, IFI/Plenum Data Company, New York 1977.
- [12] C.M. Kormanyos *et al.*, *Phys. Rev.* **C51**, 669 (1995).

- [13] T. Ericson, W. Weise, *Pions and Nuclei*, Clarendon Press, Oxford 1988.
- [14] J.N. Ginocchio, *Phys. Rev.* **C17**, 195 (1978).
- [15] E. Oset, L.L. Salcedo, *Nucl. Phys.* **A468**, 631 (1987).
- [16] M.J. Vicente Vacas, E. Oset, *Nucl. Phys.* **A568**, 855 (1994).
- [17] A. Bohr, B.R. Mottelson, *Nuclear Structure*, Vol. 1, W.A. Benjamin, Inc., 1969.
- [18] L. Stodolski, *Proc. of the Vth Intern. Coll. on Multiparticle Reactions*, Oxford 1975, p. 577.
- [19] S. Amerio *et al.* (The ICARUS Coll.), *Nucl. Instrum. Methods* **A526**, 329 (2004).
- [20] C.H. Llewellyn Smith, *Phys. Rep.* **3**, 261 (1972).
- [21] A. Rubbia “NUX- neutrino generator”, 1st Workshop on Neutrino–Nucleus Interactions in the Few GeV Region (NuInt01), Tsukuba, Japan, 13–16 Dec. 2001.